Simulate the slotline mode in coplanar waveguides using Sonnet

Xueyue Zhang and Mohammad Mirhosseini

October 20, 2017

The coupling of resonators to the slotline mode (odd mode) of the waveguide may account for a source of dissipation, which might put a limit on the achievable ratio of the external Q factor to the intrinsic Q. The purpose of this note is to study the properties of the slotline mode and its coupling with the resonator. Furthermore, we would like to propose several design guidelines to minimize the influence of the slotline mode and increase the ratio of the external/intrinsic Q ratio.

1 Different configurations

1.1 Even mode

The most common way (Cfg. 0) to simulate the even mode is to place a pair of port at the two terminals of the central strip of the waveguide. In this case, the two panels are grounded with the box but the interaction between the central strip and the two panels plays an essential role in guiding the wave.

The two alternative configurations to simulate the even mode are shown in Fig. 1 and Fig. 2. Cfg. 1 puts the ports on the panels instead of the central strip, which is now grounded. The panels in this case, not only interact with the central strip but also with the box wall (ground). Therefore, there are two paths for the current excited from the ports to flow, the central strip and the box, which correspond to the coplanar waveguide (CPW) mode (the desired even mode) and the coupled micro-stripline mode (two micro-stripline coupled together without the central strip). The total impedance turns out to be the impedance of the two modes in parallel $Z_{total} = Z_{CPW} || Z_{strip}$.

Cfg. 2 solves the above problem by adding the negative numbered ports to the central strip, which forces the current flowing from the panels to enter the central strip completely. The fringe current dissappears in this case and the characteristic impedance reaches around 50 Ω regardless of the box size.
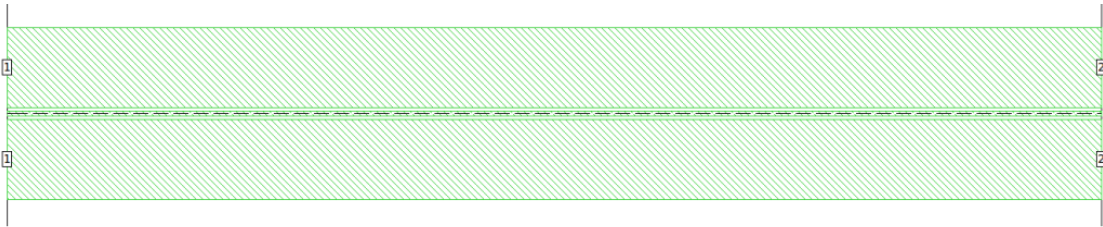

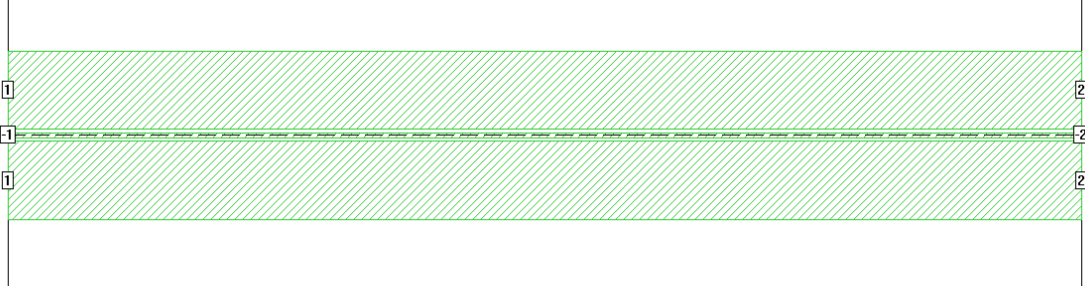**Figure** 1: Configuration 1 for even mode simulation

1

Figure 2: Configuration 2 for even mode simulation

1.2 Odd mode

Cfg. 1 for simulating the odd mode is shown in Fig. 3. The influence of the box should also be dealt with carefully, for both the central strip and the box are grounded.

Cfg. 2 (Fig. 4) is designed to eliminate the box influence inspired by the Cfg. 2 for the even modes. However, Sonnet produces a warning for this configuration stating that the positive and negative ports should not be shorted together. The corresponding results are also weird.

Cfg. 3 (Fig. 5) is physically similar to Cfg. 1 by utilizing the conductivity of the box to mirror the other half of the waveguide and excite an odd mode.
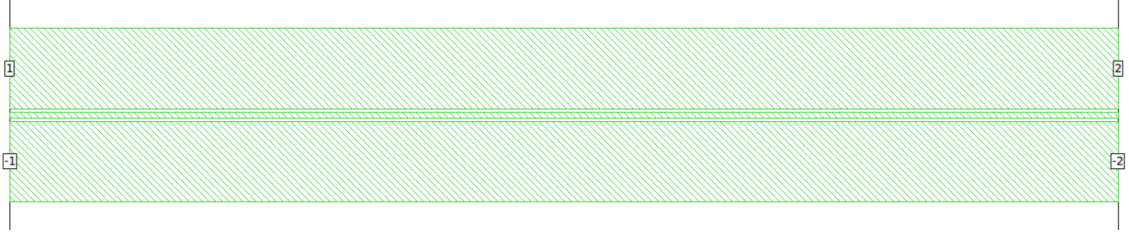

Figure 3: Configuration 1 for odd mode simulation

1.3 Comparison of the results from different configurations

For the even mode, Cfg. 0 and Cfg. 2 give almost the same results but Cfg. 1 deviates a lot especially in the impedance. For the odd mode, Cfg. 2 encounters warnings in Sonnet and the results seem unreliable in characterizing the odd mode. The dispersion curves for Cfg. 1 and 3 are similar and the impedance for Cfg. 1 is almost twice of that for Cfg. 3. It is because Sonnet calculates the differential mode Z_0 for Cfg. 1, which is twice the impedance of a single conductor [1].

2 Influence of the box size

Cfg. 1 and 3 to study the odd modes also include the interaction between the panels and the box wall. The changes in the dispersion curve is tiny therefore we use the characteristic impedance as a factor
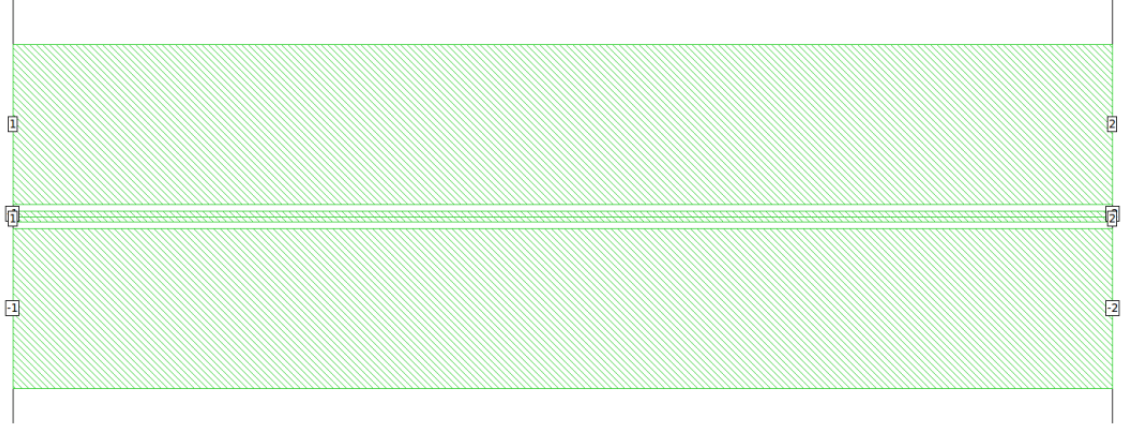
Figure 4: Configuration 2 for odd mode simulation
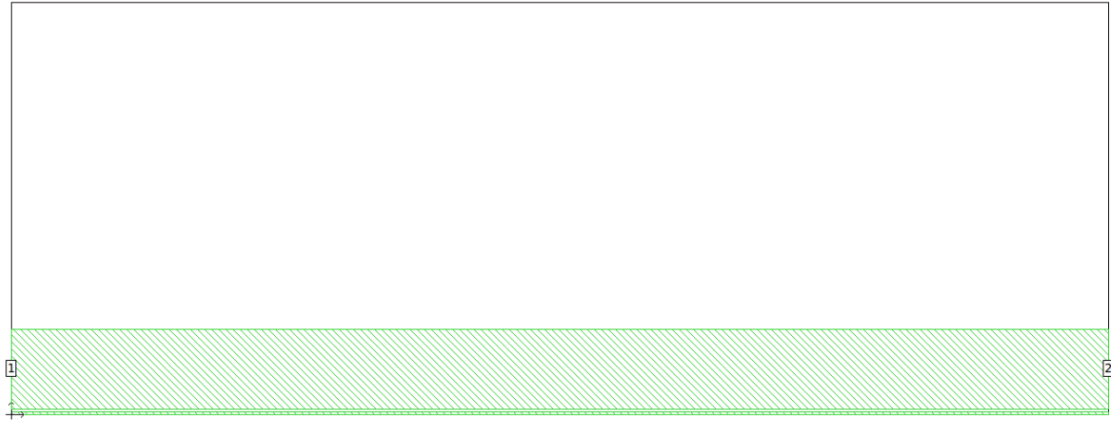

Figure 5: Configuration 3 for odd mode simulation

to study the influence of the box size. The dimension parameters used is shown in Fig. 8 and Cfg. 3 is employed to reduce the simulation scale.

The impedance convergences with a large enough size of the box in both dimensions.

The impedance of the even mode Cfg. 1 also changes with increasing size of the box, in a even more drastic way (shown in Table. 1) because the impedance of the stripline mode is related to the box size.
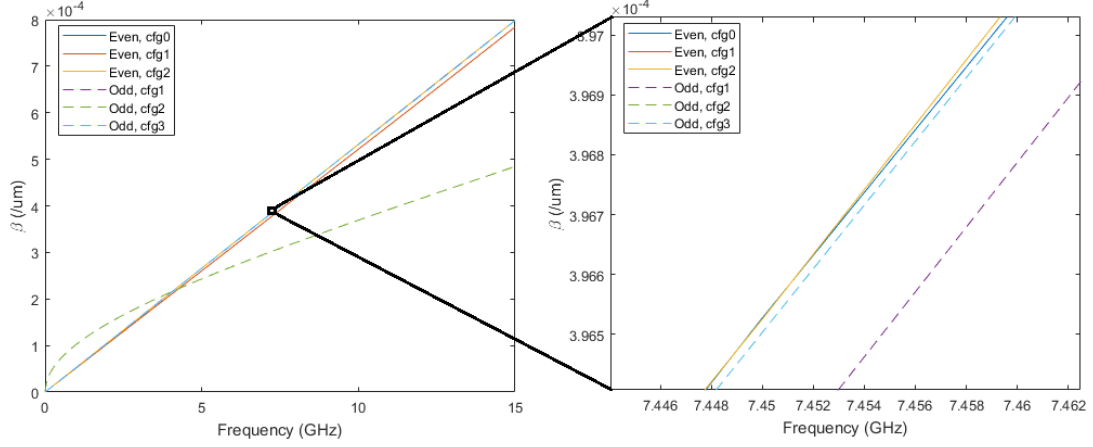
Figure 6: Dispersion relation for the above configurations. The almost overlaid curves are zoomed in.
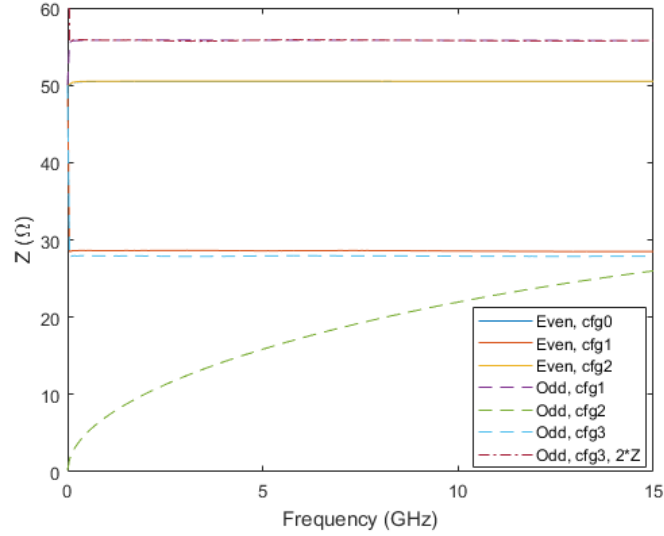

Figure 7: Characteristic impedance for the above configurations. Cfg. 0 and Cfg. 2 of the even mode are overlaid. Cfg. 1 and two times the Cfg. 3 of the odd mode are overlaid.

3   Dimension parameters of the waveguide

The three tunable dimension parameters of the waveguide is shown in Fig. 8. The whole geometry is mirrored by the box so that the width of the central strip is actually 2hWid. For the even mode, the characteristic impedance is determined mainly by hWid and gap (might because there is no current flowing on the outer rim of the panel). But for the odd mode, the width of the panel (Pwid) also matters.

4
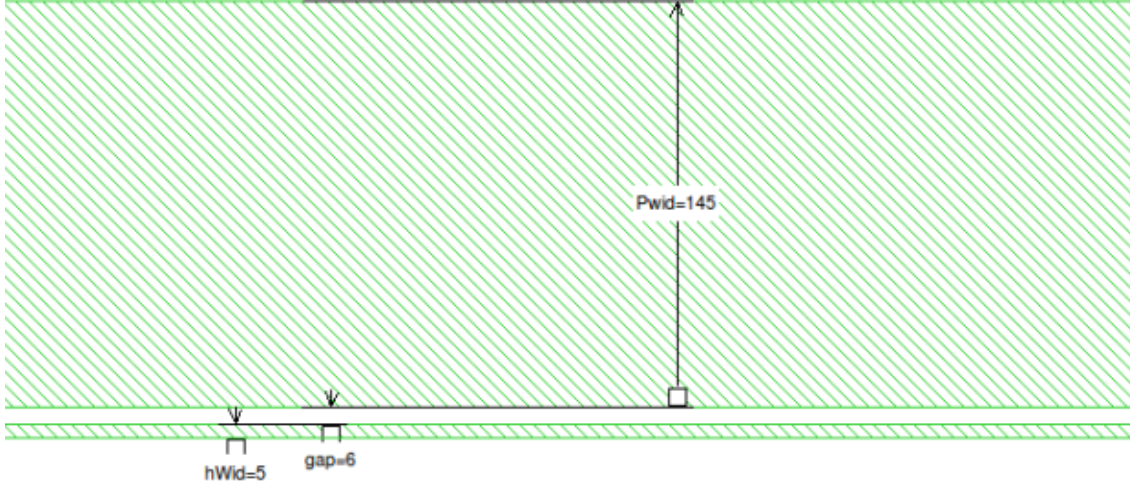
Figure 8: Dimension parameters used in studying the influence of the box size using Cfg. 3 for odd mode.
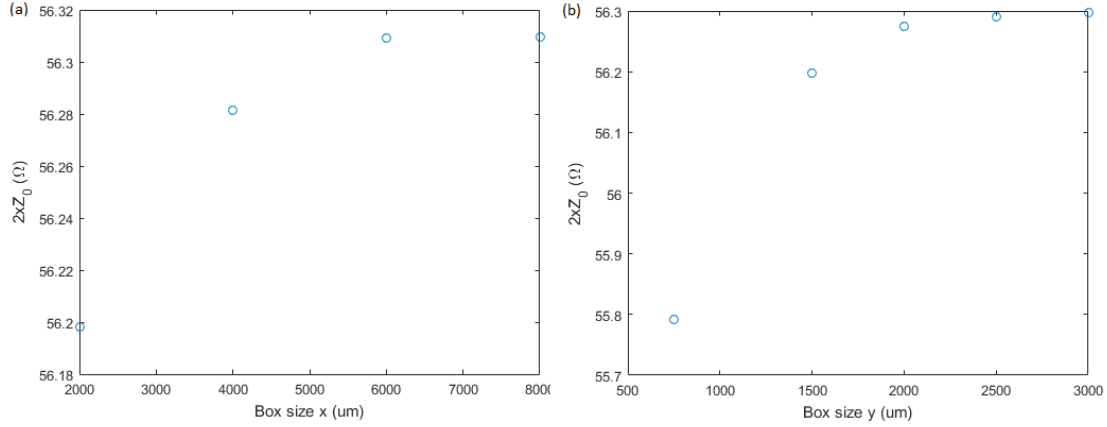

Figure 9: Characteristic impedance of the waveguide mode with (a) varying box size in the x dimension and fixed box size in the y dimension of 1500 μm; (b) varying box size in the y dimension and fixed box size in the x dimension of 2000 μm.

The impedance is also determined by the width of the central strip and the gap between the central strip and the panel. In the experiment, the impedance of the even mode should be kept to around 50 Ω in order to match the impedance with the transmission line. With an almost constant impedance for the even mode, the impedance of the corresponding structure for the odd mode is shown in Fig. 11.

5

Table 1: Characteristic impedance of Cfg. 1 for the even mode

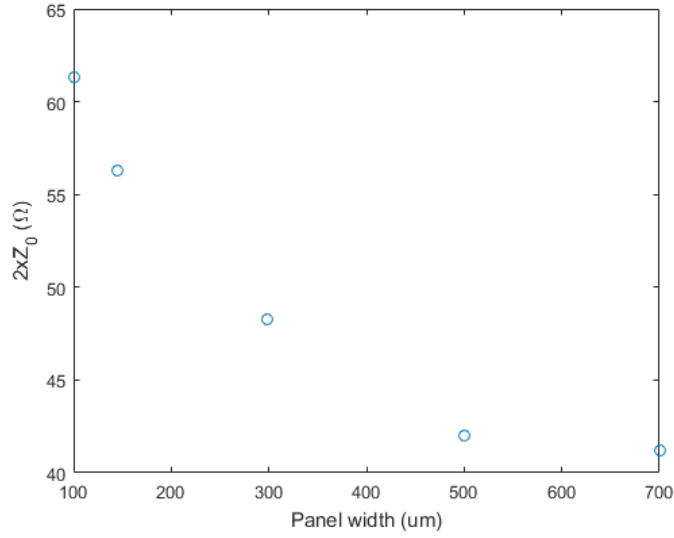| Box size (um)	2k	3k	4k	5k	6k	7k	8k	9k
1k	25.97658							
2k	30.04184							
3k	31.42586	32.38019	32.62504	32.63833				
4k	32.02657		33.6794	34.25564				
5k	32.35488							
6k	32.56564							
7k								34.63289
8k								
9k								34.94641

Figure 10: Characteristic impedance of the waveguide mode with varying panel width and fixed box size x=2000 μm and y=1500 μm. Other dimension parameters are fixed and shown in Fig. 8

4   Detection of the odd mode

We have demonstrated above how to excite odd modes in the CPW using Sonnet. The next step would be effectively detecting the odd mode, especially in the case where both the even and odd modes are present. Measuring the S_{21} parameter may help in determining the component of even/odd mode in the total wave. Use the evenly-driven port configuration as the input and the odd port configuration as the output (shown in Fig. 12), and the S_{21} parameter shows the transmitted part of the even mode through the oddly-configured ports, which is typically down to -70 dB or lower. The S_{21} for transmitted odd mode through the odd ports, on the other hand, is nearly 0 dB with matched impedance. Therefore, if a wave with the linear combination of even/odd mode transmits through the odd ports, the S_{21} indicates the portion of odd mode in the total wave.
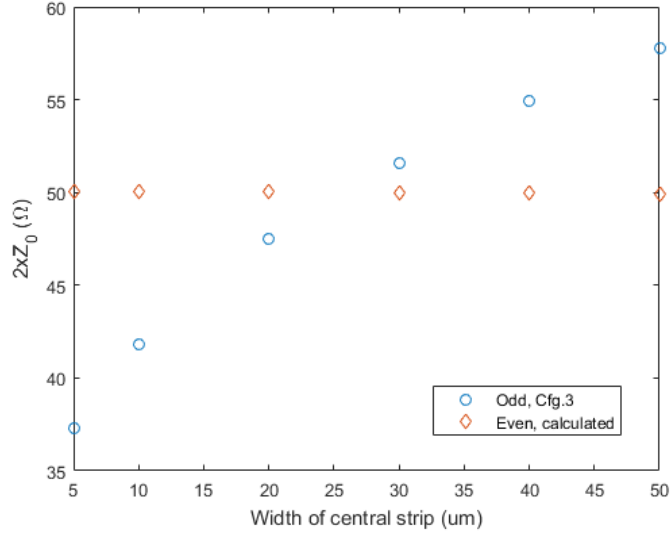
Figure 11: Characteristic impedance of the waveguide mode with varying panel width and fixed box size x=2000 μm and y=1500 μm. Other dimension parameters are fixed and shown in Fig. 8
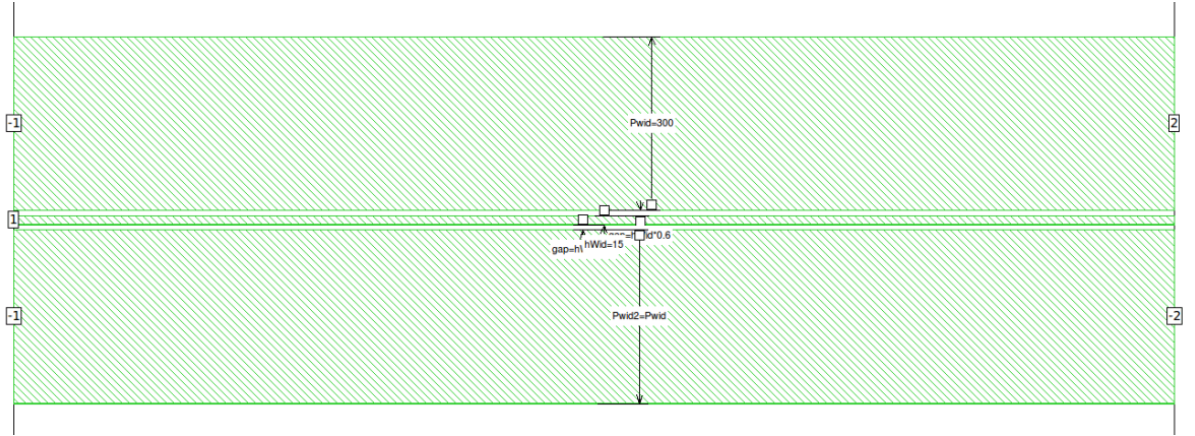

Figure 12: Port configuration for detecting the odd mode.

Unfortunately, I have not found a way in Sonnet to deterministically excite the combination of even and odd modes with a desired ratio. However, the discontinuity or asymmetry in the CPW, e.g. the unequal width of the ground planes, is known to excite odd mode [2]. Here, we use the unequal width of the ground planes in the simulation and compare the detected S_{21} with the results shown in [2]. As is shown in Fig. 13, S_{21} drops with the ratio of the ground approaching 1 as expected. We also explored the influence of the propagation distance, i.e. the length of the waveguide in the simulation, which is shown in Fig. **??**. Our simulation shows a revival of the odd mode that is not reflected from
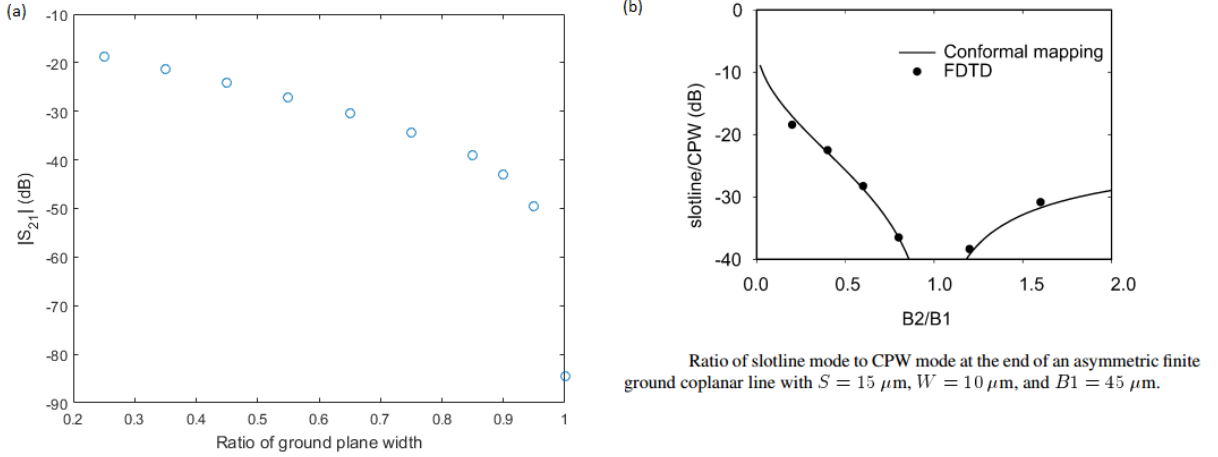
7

[2].

Figure 13: (a) Simulated S_{21} from Sonnet versus the ratio of the two ground planes with the thinner one fixed at 45 μm, the width of the central pin to be 15 μm and the gap of 9 μm. The length of the waveguide is 12 mm. (b) The result of the same geometry in [2].

5 Coupling to the resonator

Taking a step foward, we simulated the coupling between a resonator (typical quarter wavelength resoantor) to the waveguide even/odd mode, as is shown in Fig. 14. The box size is 3k by 7k (μm^2) and the width of the ground plane is 2k μm. Three different coupling methods, inductive, capacitive and directly capacitive coupling (see Fig. 15), are compared. In each cases, the coupling strength and intrinsic loss are extracted with different width of the central trace (see Fig. 16 to 21). For all of the coupling methods, the coupling to the odd mode is stronger than that to the even mode, which is believed to originate from the current distribution of the two modes. The current of even mode is highly concentrated on the central trace while the current of odd mode is more spread out in the ground plane, indicating a larger overlap with the resonator embedded in the ground plane (Fig. 22). Increasing width of the central trace, the external coupling strength increases for the even mode but decreases for the odd mode.

Similar to the detection of the odd mode in the waveguide, a hybrid port configuration is also incorporated in testing the coupling of the resonator to the waveguide mode. On the resonance, there is a large portion of even mode converted to the odd mode through the resonator (Fig. 23). Note that, the boundary reflective for one of the mode, so the scattering parameter is a result of both the coupling between even/odd mode through the resonator and the reflection and interference at the port.
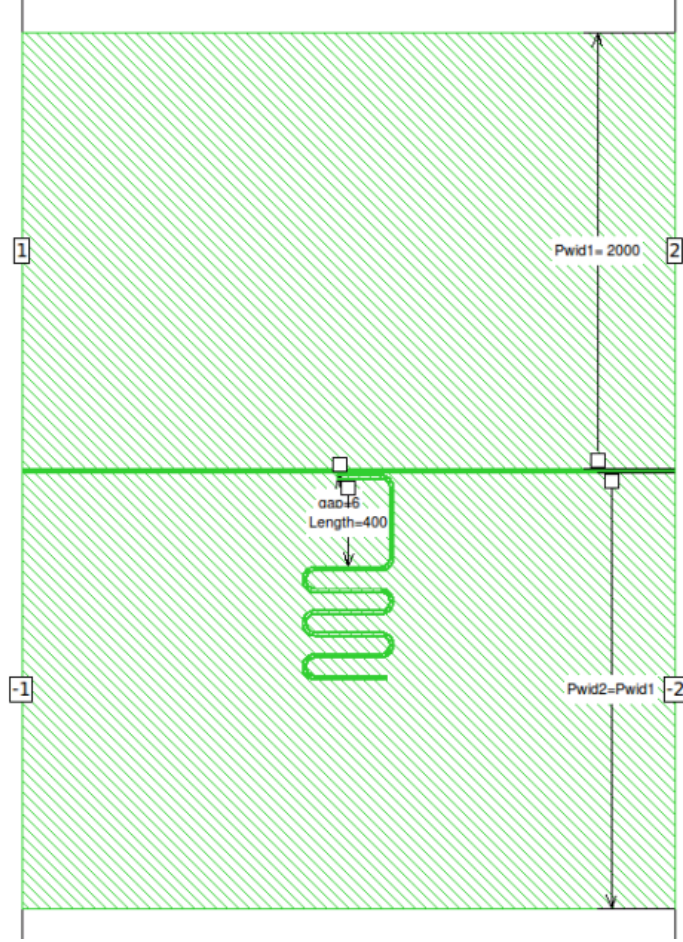
Figure 14: The geometry used to simulate the coupling between the resonator and the waveguide
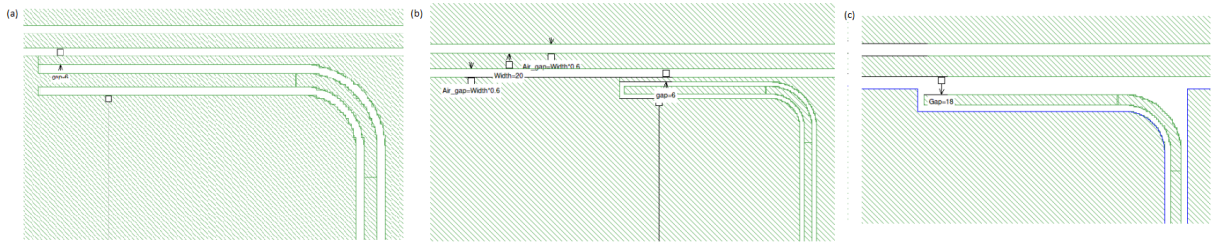

Figure 15: Three different coupling schemes between the resonator and the waveguide, and the definition of the geometric parameters. (a) Inductive coupling; (b) Capacitive coupling; (c) Direct capacitive coupling.
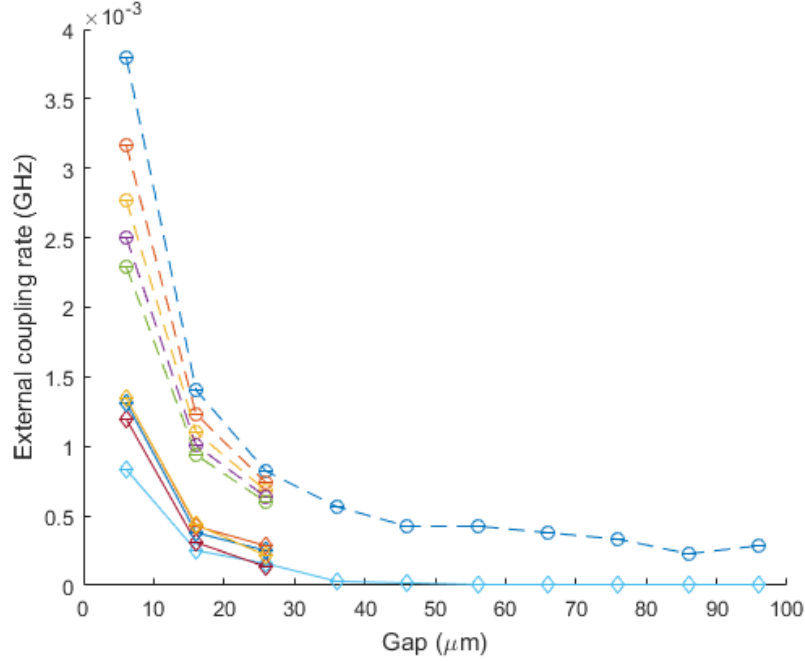
Figure 16: External coupling rate versus the gap between the inductively coupled resonator and the waveguide. The error bars (and the next five figures) represent 99% confidence interval. The coupling to the odd mode of the waveguide is shown in circles connected by dashed line and the results for even mode are shown in diamond connected by solid lines. For the odd mode, the external coupling rate decreases as the width of the central pin increases (W = 10, 20, 30, 40, 50 μm). For the odd mode, the external coupling rate increases as the width of the central pin increases (W = 10, 20, 30, 40, 50 μm). The notation of the symbols, colors and lineshape is kept the same for the next five figures.

6   Coupling to a qubit

The coupling between a qubit and the waveguide even/odd mode is also simulated. Particularly, we simulated and compared the two different configurations of qubit (namely, Xmon and transmon) in order to see the influence of different geometries (Fig. 24).

The external coupling rate and the intrinsic loss rate of the two kinds of qubit coupling with the waveguide is shown in Fig. 25 and 26. The coupling between the Xmon and the waveguide is similar to that of a resonator to the waveguide. For transmon, the coupling to the even mode is more than two times larger than that to the odd mode.

References

[1] Dima A Smolyansky and Steven D Corey. Characterization of differential interconnects from time domain reflectometry measurements. *Microwave Journal*, 43(3):68–68, 2000.
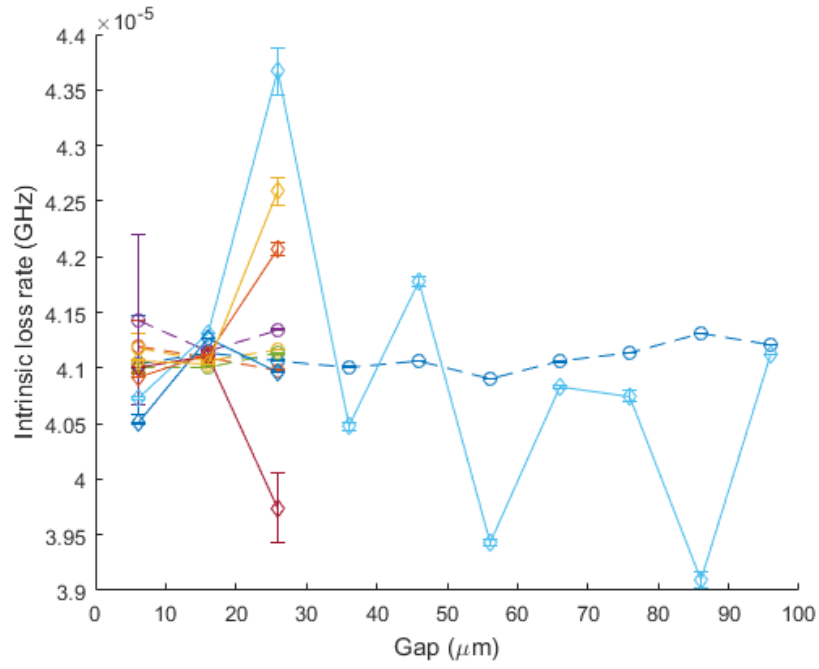
Figure 17: Intrinsic loss rate versus the gap between the inductively coupled resonator and the waveguide.

[2] George E Ponchak, John Papapolymerou, and Manos M Tentzeris. Excitation of coupled slotline mode in finite-ground cpw with unequal ground-plane widths. *IEEE transactions on microwave theory and techniques*, 53(2):713–717, 2005.
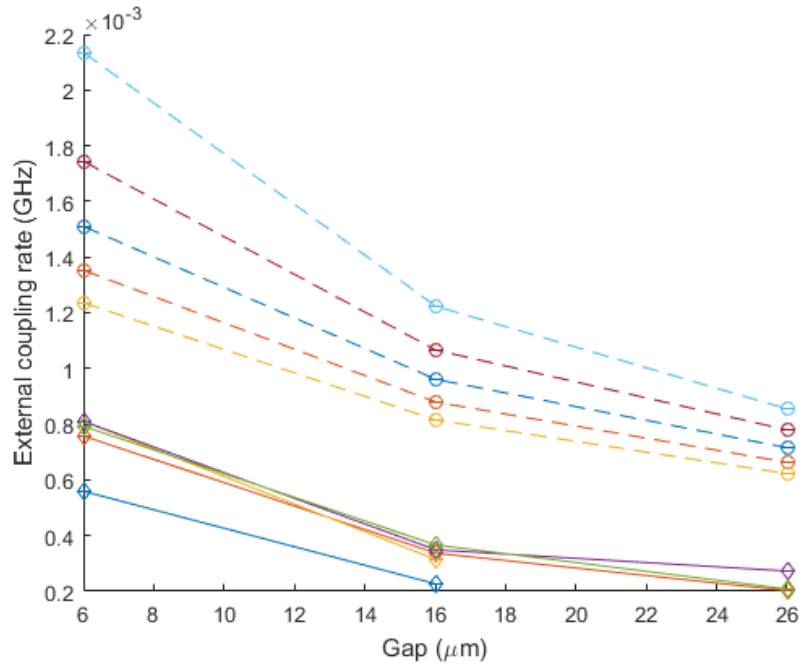
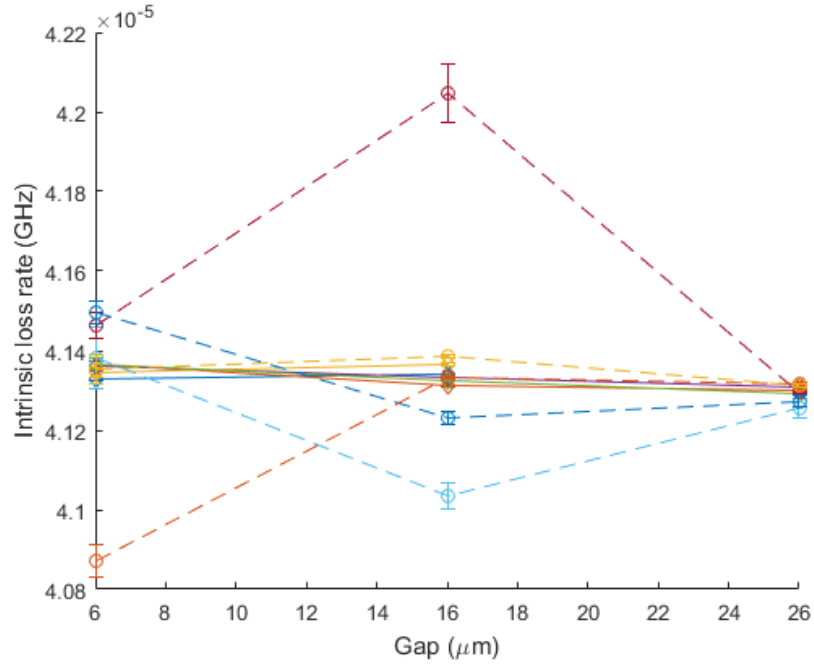**Figure** 18: External coupling rate versus the gap between the capacitively coupled resonator and the waveguide.

Figure 19: Intrinsic loss rate versus the gap between the capacitively coupled resonator and the waveguide.
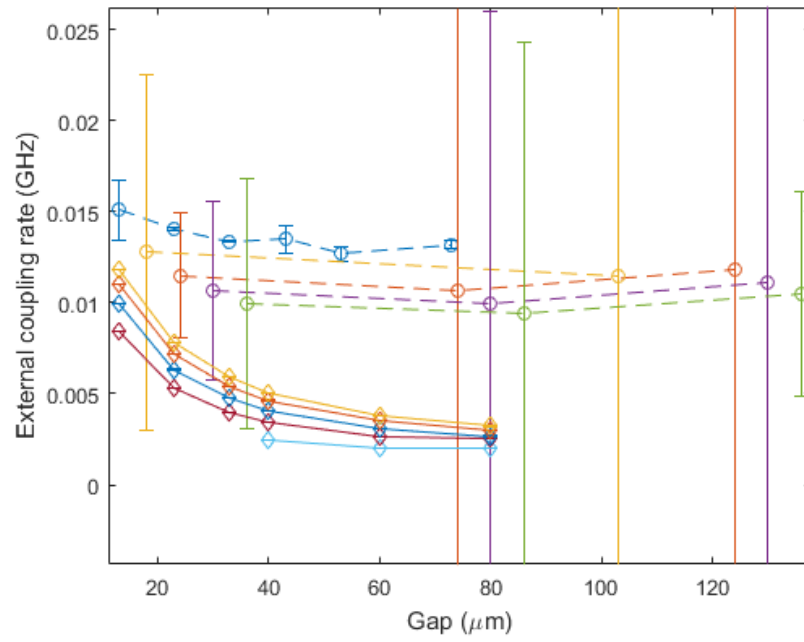
Figure 20: External coupling rate versus the gap between the directly-capacitively coupled resonator and the waveguide.
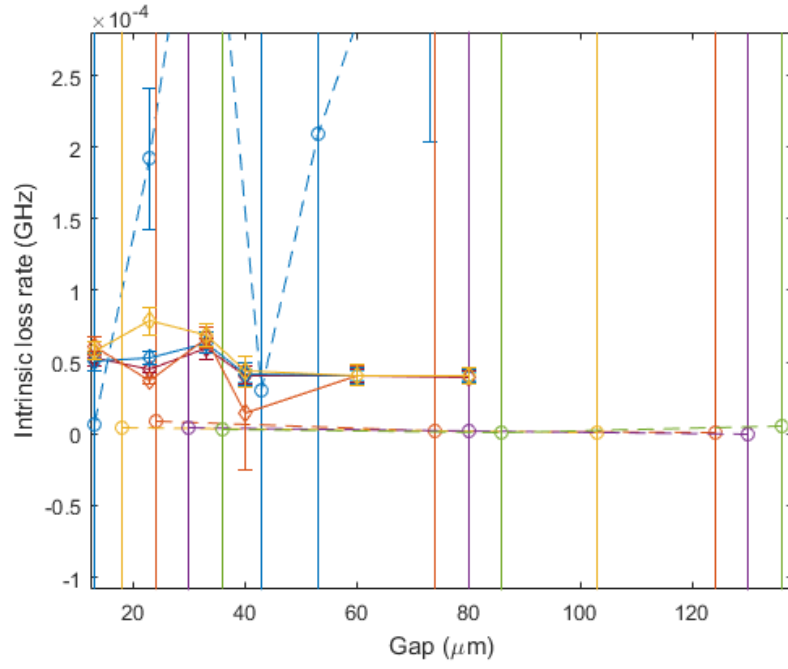
Figure 21: Intrinsic loss coupling rate versus the gap between the directly-capacitively coupled resonator and the waveguide.
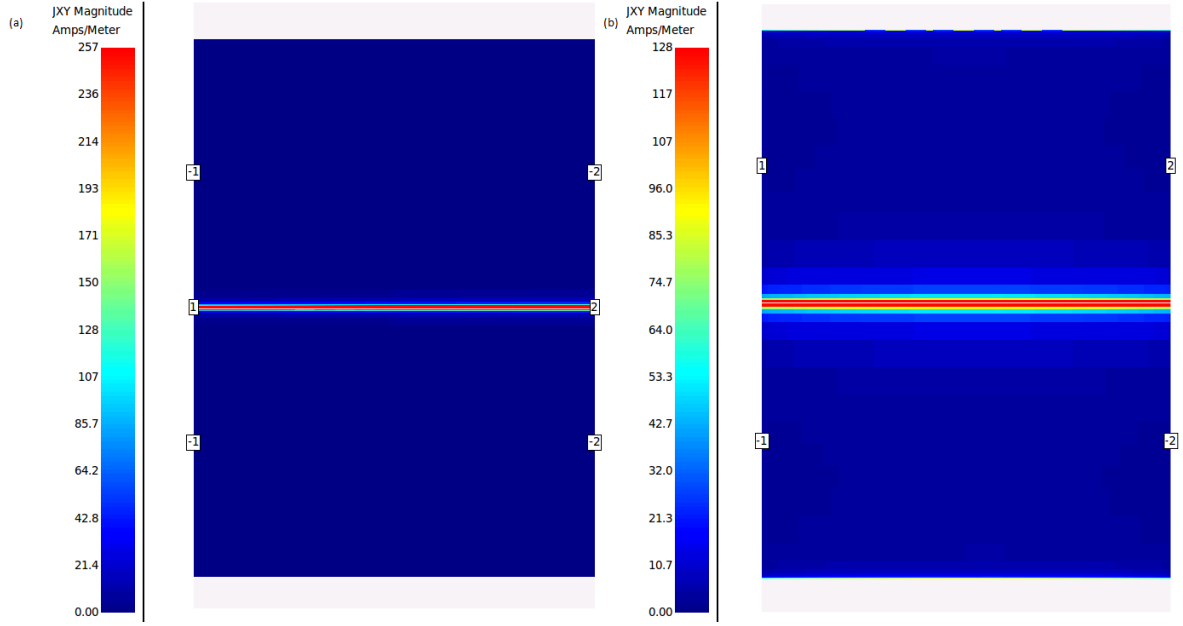
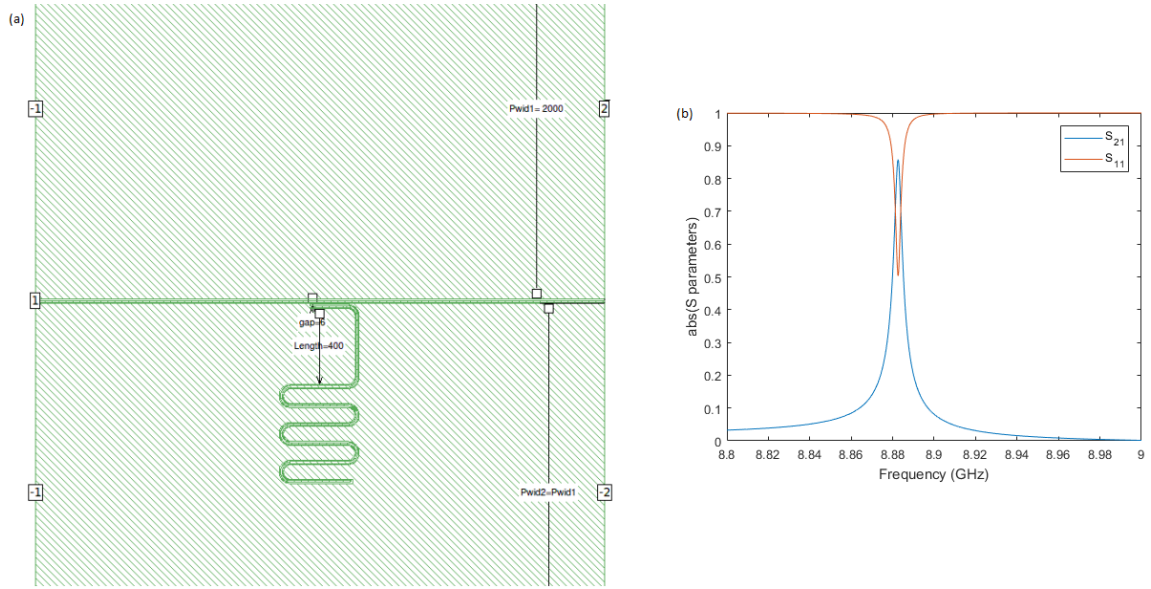**Figure** 22: The current view of waveguide excited by (a) even and (b) odd ports configuration

Figure 23: (a) Hybrid port configuration for waveguide inductively coupling with the resonator and the corresponding scattering parameters S_{21} and (b) S_{11} at gap=6 μm.
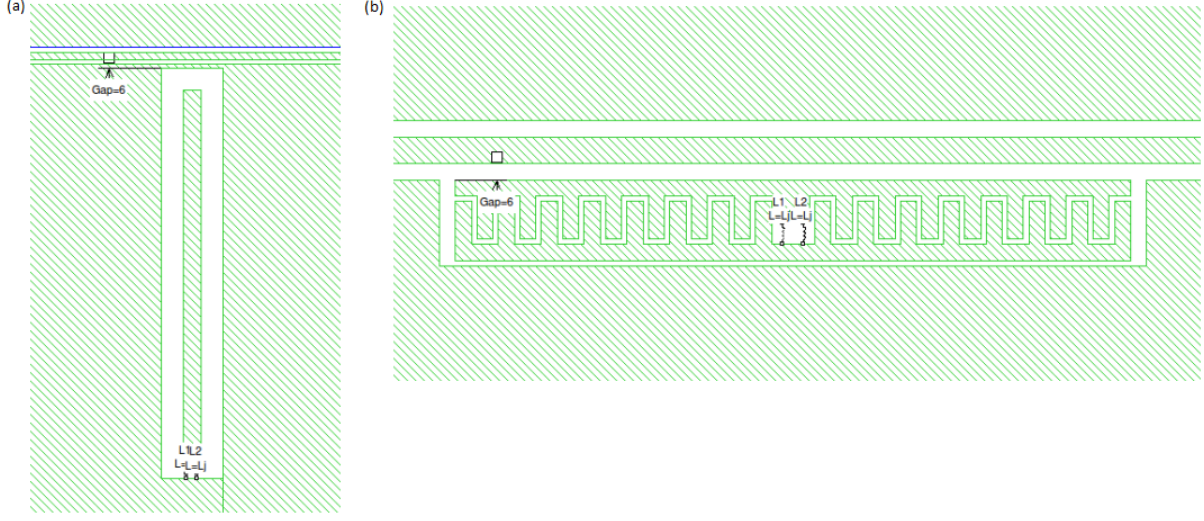
Figure 24: Geometry of coupling between (a) Xmon and (b) transmon to the waveguide. The resonance frequencies of the two qubit are set to the same at 8.8 GHz.
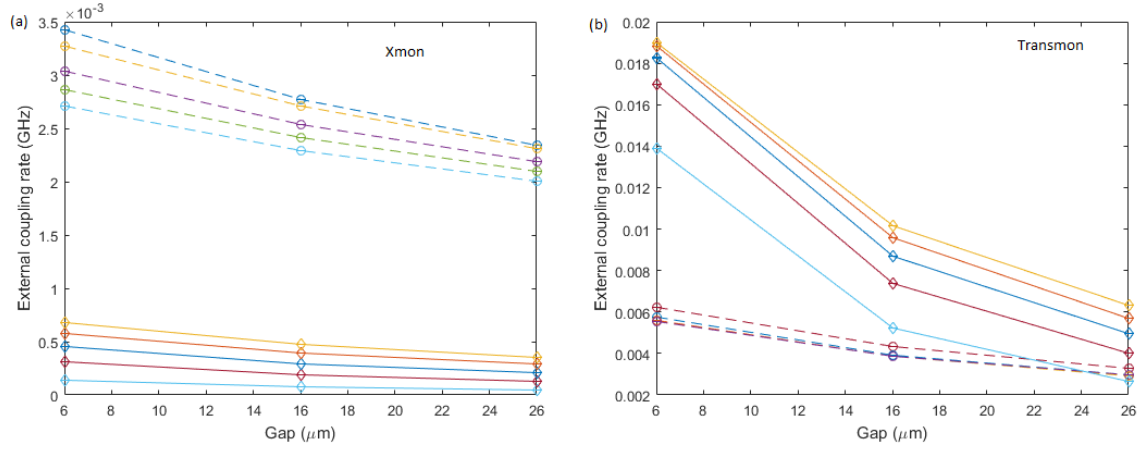

Figure 25: External coupling rate versus the gap between (a) Xmon (b) transmon and the waveguide. The error bars (and the next figure) represent 99% confidence interval. The coupling to the odd mode of the waveguide is shown in circles connected by dashed line and the results for even mode are shown in diamond connected by solid lines. For the odd mode, the external coupling rate decreases as the width of the central pin increases (W = 10, 20, 30, 40, 50 μm). For the odd mode, the external coupling rate increases as the width of the central pin increases (W = 10, 20, 30, 40, 50 μm). The notation of the symbols, colors and lineshape is kept the same for the next figure.
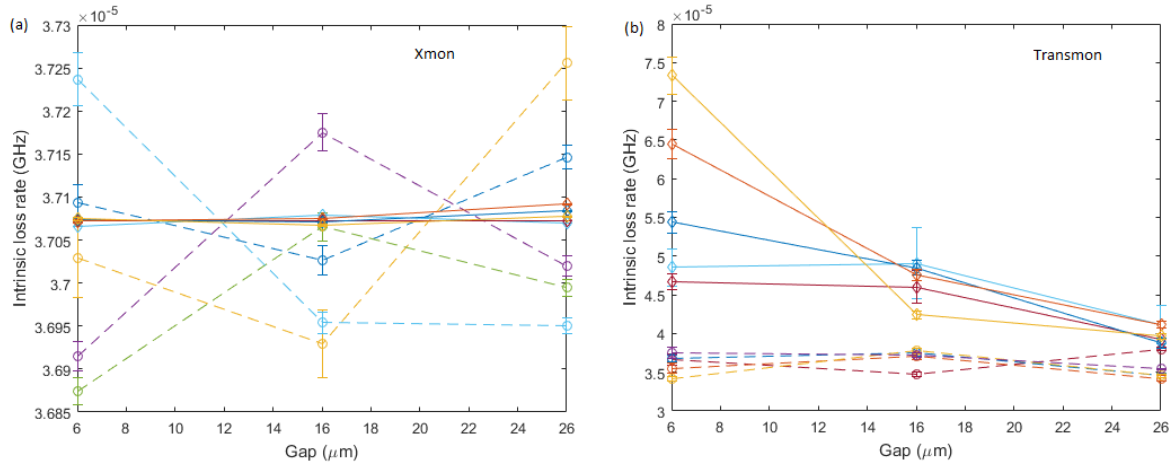
17

Figure 26: Intrinsic loss coupling rate versus the gap between (a) Xmon (b) transmon and the waveguide.